




Article

Hydroalkoxylation of Terminal and Internal Alkynes Catalyzed by Dinuclear Gold(I) Complexes with Bridging Di(N-Heterocyclic Carbene) Ligands

Elena Marcheggiani ¹, Cristina Tubaro ¹ , Andrea Biffis ¹, Claudia Graiff ²  and Marco Baron ^{1,*} 

¹ Department of Chemical Sciences, University of Padova, via Marzolo 1, 35131 Padova, Italy; elena.marcheggiani@studenti.unipd.it (E.M.); cristina.tubaro@unipd.it (C.T.); andrea.biffis@unipd.it (A.B.)

² Department of Chemistry, Life Sciences and Environmental Sustainability, University of Parma, Parco Area delle Scienze 17/A, 43124 Parma, Italy; claudia.graiff@unipr.it

* Correspondence: marco.baron@unipd.it

Received: 28 November 2019; Accepted: 14 December 2019; Published: 18 December 2019



Abstract: A series of six dinuclear gold(I) complexes with bridging bidentate N-heterocyclic carbene ligands (NHCs) of general formula $\text{Au}_2\text{Br}_2\text{L}^X$ (L = diNHC, X = 1–6) have been studied as catalysts in the intermolecular hydroalkoxylation of terminal and internal alkynes. The best catalytic results have been obtained by using $\text{Au}_2\text{Br}_2\text{L}^4$, characterized by 2,6-diisopropylphenyl wingtip substituents and a methylene bridging group between the two NHC donors. Complex $\text{Au}_2\text{Br}_2\text{L}^4$ has been structurally characterized for the first time in this work, showing the presence of intramolecular aurophilic interaction in the solid state. In the adopted reaction conditions $\text{Au}_2\text{Br}_2\text{L}^4$ is able to convert challenging substrates such as diphenylacetylene. Comparative catalytic tests by using the mononuclear gold(I) complexes AuIL^7 and IPrAuCl have been performed in order to determine the possible presence of cooperative effects in the catalytic process.

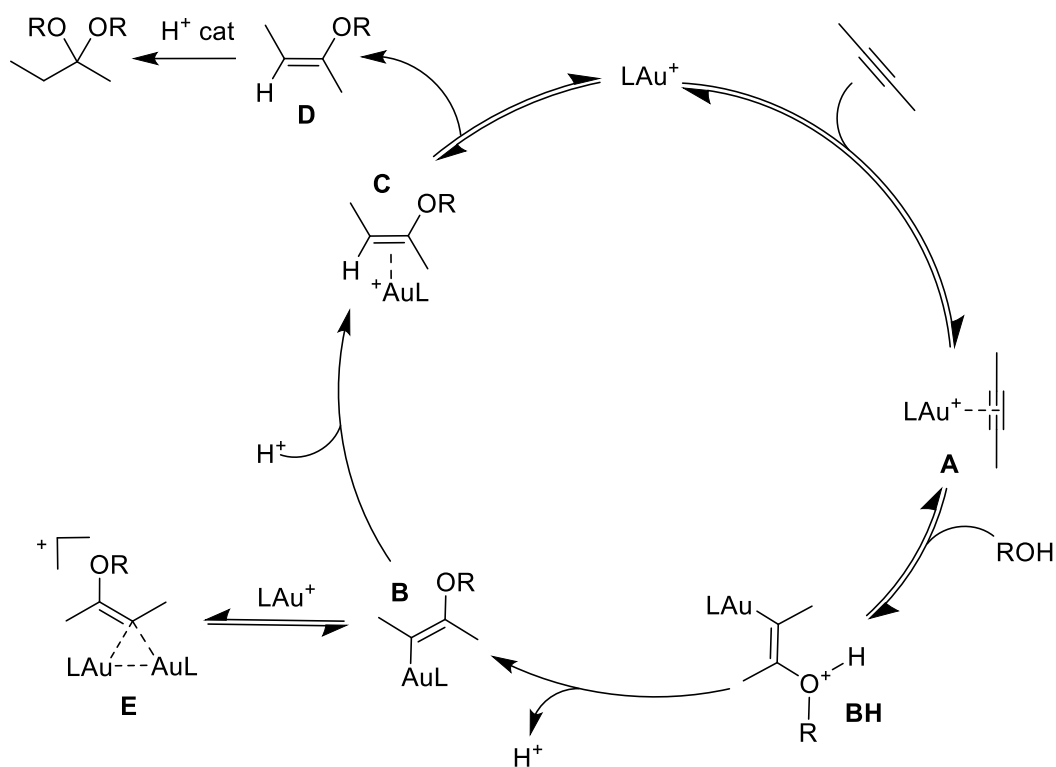
Keywords: gold(I); di(N-heterocyclic carbene) ligands; dinuclear complexes; alkynes; hydroalkoxylation; hydration

1. Introduction

Gold catalyzed hydroalkoxylation of alkynes, first reported in the late nineties [1], is an interesting 100% atom-economic reaction that allows for the preparation of vinyl ethers and acetals [2]. This reaction is conveniently catalyzed by cationic gold(I) complexes of general formula AuL^+ , usually prepared in situ, starting from the neutral species AuLX by halide abstraction with the silver AgY salt (Y = poorly coordinating anion) [3]. The resulting species in the reaction environment can easily coordinate the solvent molecule or the substrate. Ligand L is instead a spectator ligand that stabilizes the active form of the catalyst and modulates its stereoelectronic properties. Among the different available L-type ligand classes, those achieving the best performances are phosphines and N-heterocyclic carbenes (NHCs) [4–6].

The reaction mechanism depicted in Scheme 1 has been deeply studied in a seminal work by Zhdanko and Mayer [7]. The reaction starts with the formation of the alkyne π -coordinated species **A**, which subsequently undergoes a reversible *anti*-addition of an alcohol molecule leading to **BH**. The equilibrium between **A** and **BH** is shifted toward **A** because of the great tendency of **BH** to undergo 1,2 elimination. However, **BH** is also a highly acidic species and can convert into **B** via intermolecular proton transfer with the solvent. This latter step is irreversible, allowing the reaction to proceed toward product formation. Vinyl gold species **B** is highly reactive; it can undergo protonolysis, affording the π

complex **C** and subsequently the vinyl ether **D**, the final product of the gold catalyzed process together with the starting form of the catalyst. On the other hand, **B** can also react competitively, with respect to the protonolysis, with another catalyst molecule, affording the diaurated species **E**. Formation of **E** is a drawback in the catalytic process, in fact, it cannot directly undergo the protonolysis step, and it is considered an off-cycle intermediate. In this view, it is important to know that the employment of bulky L-type ligands coordinated to the gold center can reduce or even eliminate the possibility of forming **E**, increasing the catalytic performance of the system.



Scheme 1. Mechanism of the gold-catalyzed hydroalkoxylation of alkynes.

The described mechanistic picture seems to exclude a beneficial effect of dual gold catalysis in the case of the hydroalkoxylation of alkynes. The possibility for two gold centers to be part of a single catalytic cycle, known as dual gold catalysis, has been reported by several authors [8–11]. In fact, σ , π -diaurated acetylide complexes and gem-diaurated phenyl species have been recognized as catalyst reservoirs or intermediates in different gold-catalyzed processes [12,13].

In this frame, a case that partially deviates from this general trend, is represented by the hydrophenoxylation of diphenylacetylene catalyzed by the dinuclear gold(I) complex $[\{Au(IPr)_2(\mu-OH)\}][BF_4]$, studied in detail by Nolan and coworkers [14–16]. In this reaction, the gold catalyst is not only involved in the alkyne activation by forming the **A**-type π -complex (Scheme 1), but also reacts at the first stage of the reaction with phenol, forming the species $[\{Au(IPr)_2(\mu-OPh)\}]^+$, thus also activating the nucleophile [15].

Another important feature that has emerged only recently about the mechanism of the gold catalyzed hydroalkoxylation of alkynes is the role of the anionic species present in the system [17].

The halide, initially coordinated to the gold(I) center in the precatalyst $AuLX$, is replaced by the anion of the silver salt Y^- , whose coordinating ability can play an important role in the initial pre-equilibrium step (i.e., the coordination of the alkyne, step 1). However, the anion effect on the reaction does not stop here: anion basicity is another important parameter that can enhance the alcohol nucleophilicity. As reported by Zuccaccia et al., $-SO_3$ containing anions (NTf_2^- , OTf^- , OTs^- ,

and OMs[−]) characterized by an intermediate coordination ability and basicity have shown the best catalytic performances [18–21].

We have been interested for a few years in the properties of dinuclear gold(I) complexes with bridging bidentate NHC ligands (μ -diNHC) [22]. An interesting feature of this class of compounds is the possible presence of intramolecular aurophilic interaction, usually supported by the bridging diNHC ligand [23,24]. When present, aurophilicity can deeply modify the properties of the system, promoting high quality photoemission properties [25–29], and imparting new reactivity of the complexes (e.g., in the oxidative addition of halogens, favoring the formation of gold(II) dinuclear complex with a covalent gold(II)-gold(II) bond) [30–33]. More recently, we have also started to investigate the possible influence of this interaction in promoting cooperative effects in the catalytic properties of dinuclear gold(I) complexes of general formula $\text{Au}_2\text{Br}_2(\mu\text{-diNHC})$ [34]. In the hydroamination of terminal alkynes, we have observed that complexes presenting among their structural feature the shortest gold(I)⋯gold(I) distance afford the best catalytic performances, suggesting the presence of possible beneficial cooperative effects [34]. In this work, we wanted to extend our catalytic study by investigating the hydroalkoxylation of alkynes. A family of six different dinuclear gold(I) diNHC complexes were tested and compared with two mononuclear gold(I) NHC complexes.

2. Results and Discussion

2.1. Screening of the Reaction Conditions

We have recently reported on the synthesis of a family of dinuclear gold(I) complexes of general formula $\text{Au}_2\text{Br}_2\text{L}$ (L = diNHC) (Figure 1) and their catalytic activity in the hydroamination of terminal alkynes with anilines [34]. Here, we have extended the catalytic investigation by studying the hydroalkoxylation of alkynes with aliphatic alcohols (Scheme 2).

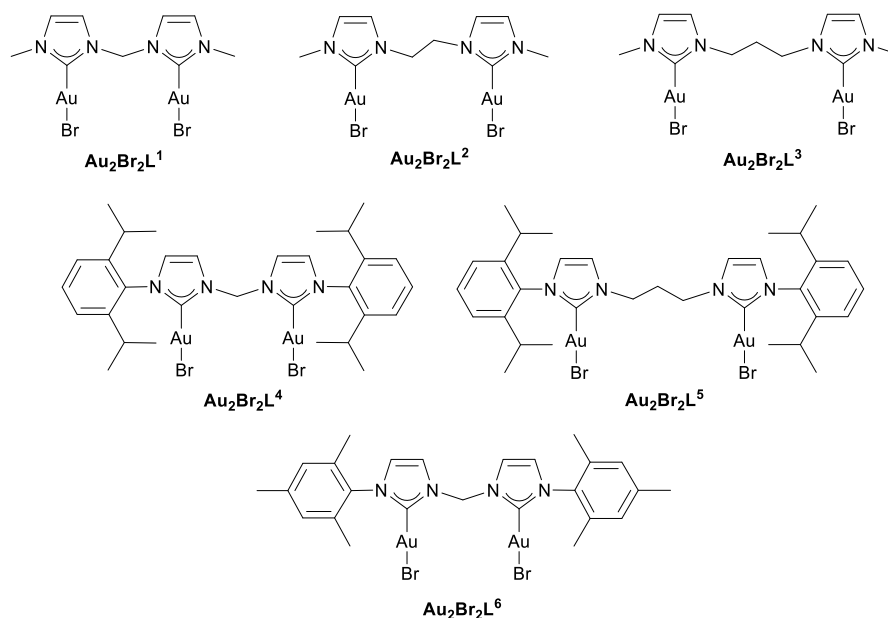
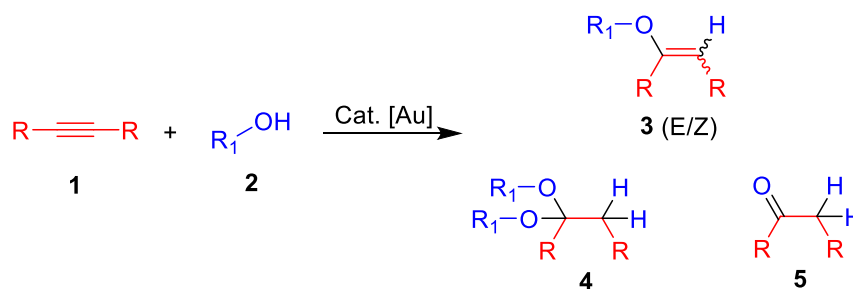


Figure 1. Family of dinuclear gold(I) complexes with bridging diNHC ligands used in this study.

In the reaction of alkynes with alcohols, different products may form: the addition of a single alcohol molecule leads to an *E* or *Z* vinyl ether (Scheme 2, Product 3); the addition of a second alcohol molecule leads to the acetal (Scheme 2, Product 4); and finally hydrolysis of the acetal, usually due to traces of water present in the system, gives the hydration product (Scheme 2, Product 5). It is important to remark that while the formation of the vinyl ethers is a gold catalyzed process, the addition of the second alcohol molecule is considered to be a classical proton-catalyzed process [7]. The selectivity of

the system is determined by different factors and can be tuned by modifying the adopted reaction condition, depending on the desired product [35]. The ketones obtained upon acetal hydrolysis are also valuable products and the alcohol route, with the on-purpose addition of one equivalent of water for promoting the hydrolysis, is among the most efficient synthetic strategy to obtain these products starting from alkynes [36,37]. Considering the rather complex mixture that is possible to obtain in the hydroalkoxylation of alkynes, the complexity of which can be even enhanced by using nonsymmetric alkynes, the catalytic performances of the complexes used herein have been initially ranked based only on the achieved alkyne conversion. Product selectivity will be discussed only for the reactions performed under optimized conditions.



Scheme 2. Products of the hydroalkoxylation of a symmetric alkyne.

We started our investigation by screening the reaction conditions in terms of reaction solvent, temperature and silver co-catalyst employed to remove the bromides coordinated to the gold(I) centers.

After some preliminary experiments, we selected the hydromethoxylation of ethyl phenylpropiolate as the reference system for carrying out the optimization work (Table 1). It turned out that the reaction can be conveniently performed under neat conditions, using the alcohol in excess as a solvent, although the use of a non-coordinating solvent like chloroform is not detrimental. In contrast, the use of a solvent with good coordinating properties like acetonitrile, significantly decreases the conversion of the alkyne. Moderate heating (40 °C) is necessary to promote the reaction. Finally, the anion present in the system does not dramatically affect the catalytic performance of the gold(I) complexes (Entries 2 and 5). We decided to use AgOTf as the silver co-catalyst to better compare our results with those reported in the hydroalkoxylation reaction by Zuccaccia et al. [19–21], considering that they did not use the hexafluoroantimonate anion.

Table 1. Selected experiments performed during the screening of the reaction conditions.

Entry	Solvent	Cat	Co-Cat	T (°C)	t (h)	Alkyne Conversion (%) ^a
1	neat	Au₂Br₂L⁵	AgSbF ₆	rt	22	nr
2	neat	Au₂Br₂L⁵	AgSbF ₆	40	1	100
3	neat	Au₂Br₂L³	AgOTf	rt	22	nr
4	neat	Au₂Br₂L⁵	AgOTf	40	1.5	86
					18.5	89
5	neat	Au₂Br₂L³	AgOTf	40	1	62
					6.5	86
					22	87
6	CHCl ₃	Au₂Br₂L⁵	AgOTf	40	1	100
7	CH ₃ CN ^b	Au₂Br₂L³	AgOTf	40	1	<1
					22	12
8	neat	-	AgOTf	40	22	nr

Reaction conditions: Ethyl phenylpropiolate (0.6 mmol), MeOH (0.5 mL, 12.3 mmol), **Au₂Br₂L** (0.006 mmol), silver co-cat. (0.012 mmol). ^a Alkyne conversion has been determined by ¹H NMR. ^b MeOH (0.15 mL, 3.6 mmol), solvent (0.35 mL).

2.2. Catalyst Screening

With the optimized conditions in hand, we tested different dinuclear gold(I) complexes in the catalytic hydromethoxylation of ethyl phenylpropiolate with the aim of evaluating the possible ligand effects on the catalyst performance (Table 2 and Table S2). The used bidentate diNHC ligands differed for the length of the bridging group between the two carbene donors and for the steric hindrance of the wingtip substituents (Figure 1).

Table 2. Catalysts screening in the hydromethoxylation of ethyl phenylpropiolate.

Entry	Cat (mol%)	t (h)	Alkyne Conversion (%) ^a
1	Au₂Br₂L¹	1.5	67
		6.5	91
		22	92
2	Au₂Br₂L²	1.5	78
		6.5	90
3	Au₂Br₂L³	1.5	62
		6.5	86
		22	87
4	Au₂Br₂L⁴	1	100
		18.5	100
5	Au₂Br₂L⁵	1	86
		18.5	89
6	Au₂Br₂L⁶	1	72
		23	100

Reaction conditions: Ethyl phenylpropiolate (0.6 mmol), MeOH (0.5 mL, 12.3 mmol), **Au₂Br₂L** (0.006 mmol), AgOTf co-cat. (0.012 mmol), 40 °C. ^a Alkyne conversion has been determined by ¹H NMR; the yields in the different products are reported in Table S2 in the Supplementary Materials.

From the results reported in Table 2, it is possible to note that there is an important effect of the nature of the wingtip substituent on the activity of the complexes. This seems to be particularly related to the steric hindrance of the wingtip substituents. Complexes bearing 2,6-diisopropylphenyl wingtips (**Au₂Br₂L⁴** and **Au₂Br₂L⁵**) were the most active, affording the highest alkyne conversion values after one reaction hour. Most notably, complex **Au₂Br₂L⁴** was able of fully convert the substrate in one hour (Table 2, Entry 4). Complexes bearing methyl wingtips (**Au₂Br₂L¹**, **Au₂Br₂L²**, and **Au₂Br₂L³**) showed similar performances between them and were not able to fully convert the alkyne even at a long reaction time. Finally, complex **Au₂Br₂L⁶**, bearing mesityl wingtips, showed an intermediate performance with respect to the complexes bearing 2,6-diisopropylphenyl or methyl wingtips, affording a 73% conversion after 1 h and a full conversion at a longer reaction time (Table 2, Entry 6).

Another important structural parameter that can affect the catalytic behavior of the complexes is the bridging group between the two carbene donors. In the analyzed complexes, this linker was an aliphatic chain of different lengths and a methylene (**Au₂Br₂L¹**, **Au₂Br₂L⁴** and **Au₂Br₂L⁶**), di-methylene (**Au₂Br₂L²**), or tri-methylene (**Au₂Br₂L³** and **Au₂Br₂L⁵**) group. The best results were obtained with complexes bearing the shortest bridges (i.e., **Au₂Br₂L⁴** and **Au₂Br₂L⁶**), the only ones able of fully converting the substrate. Regarding the effect of the ligand features on the catalytic performance of the complexes, the best combination was achieved by merging a methylene bridging group together with a bulky 2,6-diisopropylphenyl wingtip substituent, as present in the structure of catalyst **Au₂Br₂L⁴**.

Quite surprisingly, the results obtained in this work seem to be inconsistent with what we observed in our previous studies on the hydroamination of alkynes. [34] In that case, in fact, complexes with less hindered methyl wingtip groups were more active than complexes with bulkier 2,6-diisopropylphenyl or mesityl wingtip groups. Moreover, complexes with a more flexible tri-methylene bridging group showed higher activity because of the possible presence of cooperative effects. The tri-methylene bridging group in fact, possessed the right length and flexibility to maximize the approach of the two

gold(I) centers in dinuclear complexes. Even in the case of the hydroamination of alkynes, however, when it was necessary to work under harsher conditions (higher temperatures) in order to react poorly activated substrates, the only active catalyst was $\text{Au}_2\text{Br}_2\text{L}^4$. This finding led us to consider that the optimal structural features of the catalyst to achieve maximum catalytic performance in the two reactions are different, and that in the case of the hydroalkoxylation of alkynes, the robustness of the active catalyst form is a key parameter. This can be due to the worse coordinating ability and higher reducing power of alcohols compared to amines, so that in the reaction environment, deactivation pathways leading to colloidal gold may have a higher incidence. The ease by which the two gold(I) centers can come in close contact and consequently act cooperatively appears, instead, to be much less important when compared with the stability issue outlined above. Consequently, we can state that cooperative effects in the case of the present reaction appear negligible at the present stage.

2.3. X-ray Structure Analysis

Complex $\text{Au}_2\text{Br}_2\text{L}^4$ delivered the best catalytic performance in the hydroalkoxylation of alkynes among the dinuclear gold(I) complexes used in this work. This complex was recently reported by some of us [34], although it has not been structurally characterized so far. Considering our interest in relating the catalytic performance of a catalyst to its molecular features, we decided to structurally characterize $\text{Au}_2\text{Br}_2\text{L}^4$ with single crystal x-ray diffraction analysis. Suitable crystals have been obtained by the slow diffusion of *n*-hexane into a chloroform solution of the complex. The structure consists, as expected, of a dinuclear gold(I) complex with a bridging diNHC ligand (Figure 2). The two gold(I) centers are dicoordinated by an NHC donor and a bromide in an almost linear fashion, as expected for a heavy metal center in a d^{10} electronic configuration; the C–Au–Br angles are in fact 173.5 (2) and 175.4 (2). The $C_{\text{carbene}}\text{–Au}$ and Au–Br bond distances agree with the literature values for similar compounds. [34] Interestingly, the Au1...Au2 distance of 3.2595 (5) Å suggests the presence of intramolecular aurophilic interaction, at least in the solid state. The C1–Au1–Au2–C13 dihedral angle of 45.6 (3) ° and the dihedral angle between the two NHC rings of 80.4 (4) ° indicate that the two $C_{\text{carbene}}\text{–Au}$ fragments point toward the same direction (*syn*), but deviate slightly from a parallel arrangement.

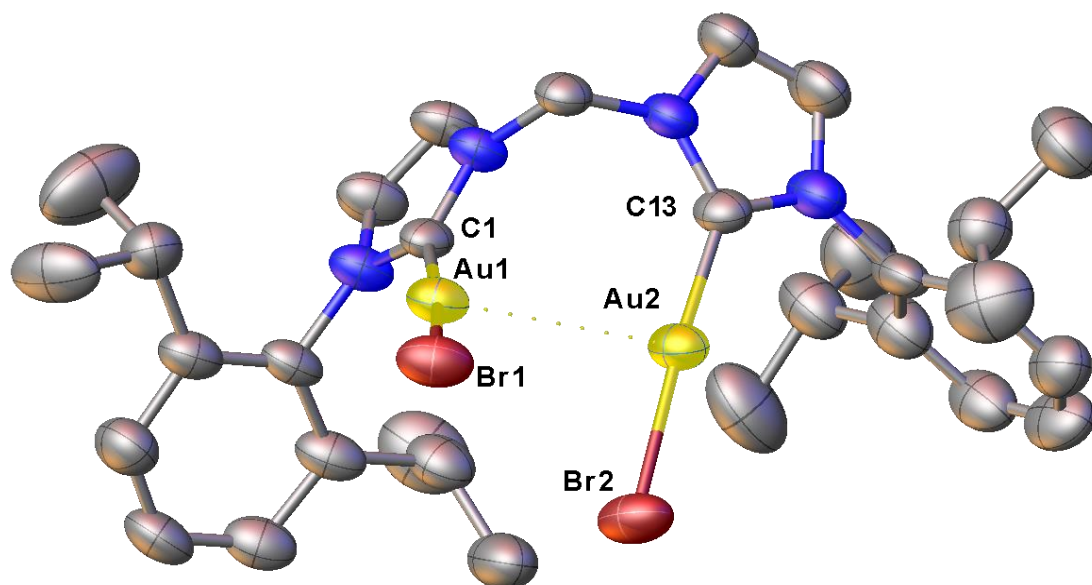


Figure 2. Oak Ridge Thermal Ellipsoid Plot (ORTEP) style view of complex $\text{Au}_2\text{Br}_2\text{L}^4$. Chloroform and *n*-hexane solvent molecules have been omitted for clarity. Thermal ellipsoids are drawn at the 50% probability level. Selected bond distances (Å) and angles (°): C1–Au1 1.989 (8), Au1–Br1 2.4079 (9), C13–Au2 1.976 (8), Au2–Br2 2.4026 (10), Au1...Au2 3.2595 (5), C1–Au1–Br1 173.5 (2), C13–Au2–Br2 175.4 (2).

Concerning the possible implications of $\text{Au}_2\text{Br}_2\text{L}^4$ structural features on its catalytic performances, the combination of bulky wingtip substituents together with the contribution of aurophilic interaction can combine, giving the complex an enhanced robustness compared to the other dinuclear complexes studied in this work.

2.4. Substrates Scope and Analysis of the Selectivity in the Hydroalkoxylation of Alkynes

We then studied the reaction scope of the hydroalkoxylation of alkynes with the best catalyst $\text{Au}_2\text{Br}_2\text{L}^4$ in the presence of AgOTf as the co-catalyst (Table 3). *n*-BuOH and PhOH were used instead of MeOH in the reaction with ethyl phenylpropiolate (Entries 2 and 3, Table 3), observing only a slightly lower efficiency for the system at the shortest reaction time, while the conversion of the alkyne was complete after 18.5 h. Interestingly, with PhOH, the hydroalkoxylation product **3ac** was the main product at the shortest reaction time and could also be observed at longer reaction times.

Table 3. Substrate scope and product selectivity in the hydroalkoxylation of alkynes catalyzed by $\text{Au}_2\text{Br}_2\text{L}^4$.

Entry	Alkyne	Alcohol	t (h)	Alkyne Conversion (%) ^a	Yield (%) ^a
1	PhC≡CCO ₂ Et	MeOH	1	100	(<i>E</i>)- 3aa (33); 5a (67)
			18.5	100	5a (100)
2	PhC≡CCO ₂ Et	<i>n</i> -BuOH	1	92	(<i>Z</i>)- 3ab (21); (<i>E</i>)- 3ab (16);
			18.5	100	5a (55) 5a (100)
3 ^b	PhC≡CCO ₂ Et	PhOH	1	66	(<i>Z</i>)- 3ac (37); 5a (29)
			18.5	100	(<i>Z</i>)- 3ac (31); 5a (69)
4	PhC≡CH	MeOH	1	66	5b (66)
			18.5	99	5b (99)
5	HC≡CCO ₂ Et	MeOH	1	50	(<i>Z</i>)- 3ca (15); (<i>E</i>)- 3ca (19);
			18.5	100	3ca' (10); 4ca (6) (<i>E</i>)- 3ca (26); 4ca (50); 5c (14)
6	EtC≡CEt	MeOH	1	58	5d (58)
			18.5	89	5d (89)
7	PhC≡CPh	MeOH	1	11	5e (11)
			18.5	63	5e (63)
8	PhC≡CCO ₂ H	MeOH	1	25	5b (14); 5g (6); 1g (5)
			18.5	50	5b (37); 5g (3); 1g (10)
9 ^c	PhC≡CPh	MeOH	1	25	(<i>Z</i>)- 3ea (21); 5e (4)
			18.5	83	5e (83)

Reaction conditions: Alkyne (0.6 mmol), MeOH (0.5 mL, 12.3 mmol), $\text{Au}_2\text{Br}_2\text{L}^4$ (0.006 mmol), AgOTf co-cat. (0.012 mmol), 40 °C. ^a Alkyne conversion and product yields has been determined by ¹H NMR; ^b Alkyne (0.6 mmol), PhOH (3.6 mmol), $\text{Au}_2\text{Br}_2\text{L}^4$ (0.006 mmol), AgOTf co-cat. (0.012 mmol), chloroform (0.5 mL), 40 °C. ^c AgOTf was used as the co-catalyst instead of AgOTf.

We then tried different alkynes, both terminal (phenylacetylene and ethylpropiolate) and internal ones (3-hexyne, diphenylacetylene and phenylpropiolic acid) in the reaction with MeOH. We did not observe a dramatic change in reactivity between terminal and internal alkynes; this is consistent with the literature data by other groups with phosphine gold(I) complexes [4], but it substantially deviates from the reactivity reported for the dinuclear gold(I) complexes $\text{AuX}_2(\text{diNHC})$ in other hydrofunctionalization reactions of alkynes such as hydroamination [34]. The activation of terminal alkynes with these catalysts is usually much easier than the corresponding reaction with internal alkynes; this remark may be indicative of a different rate determining step in the catalytic cycle. Ethyl phenylpropiolate (Entry 1, Table 3) reacted much faster than both phenylacetylene and ethyl propiolate

(Entries 4 and 5, Table 3). On the other side, 3-hexyne, diphenylacetylene, and phenylpropionic acid reacted slightly slower than the two previously mentioned terminal alkynes and, more importantly, were not fully converted even at longer reaction times (Entries 6–8, Table 3).

This might be explained by considering the different substituent groups on the alkyne: the presence of an electron withdrawing group such as the ester CO_2Et favors the nucleophilic attack to the triple bond. In contrast, with 3-hexyne, both substituents are electron donating groups (Et), and this reduces the reactivity of the alkyne toward the alcohol. Steric reasons could account for the low conversion observed with diphenylacetylene. As depicted in Scheme 2, the hydroalkoxylation of alkynes can afford different products. The selectivity is driven, first of all, by thermodynamic factors (i.e., the relative stability of the vinyl ether formed as mono-hydroalkoxylation product (Product 3, Scheme 2)) compared to the that acetals formed after the addition of a second alcohol molecule (Product 4, Scheme 2). Obviously, working with an excess of alcohol speeds up the reaction but inevitably favors the formation of the acetal. Once formed, the acetal can be hydrolyzed in the presence of water to the corresponding aldehyde or ketone. It has to be remarked that traces of water were present in the system due to reagents (alcohol and alkyne), to the hygroscopic nature of the silver salts used as co-catalyst, and to the water content in the deuterated chloroform used in the Nuclear Magnetic Resonance (NMR) experiments for evaluating the reaction outcome. The products detected in our catalytic experiments are reported in Figure 3.

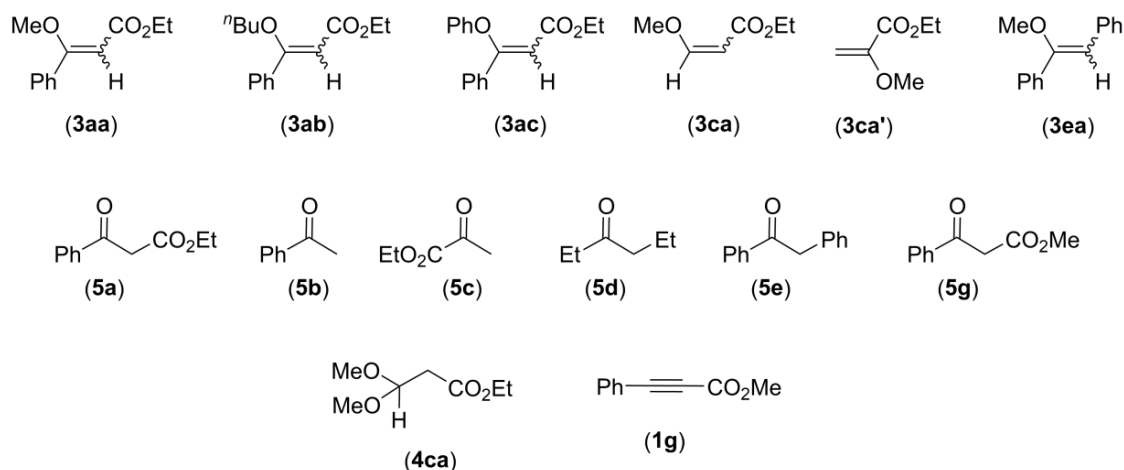


Figure 3. Products identified in the catalytic test reported in Table 3.

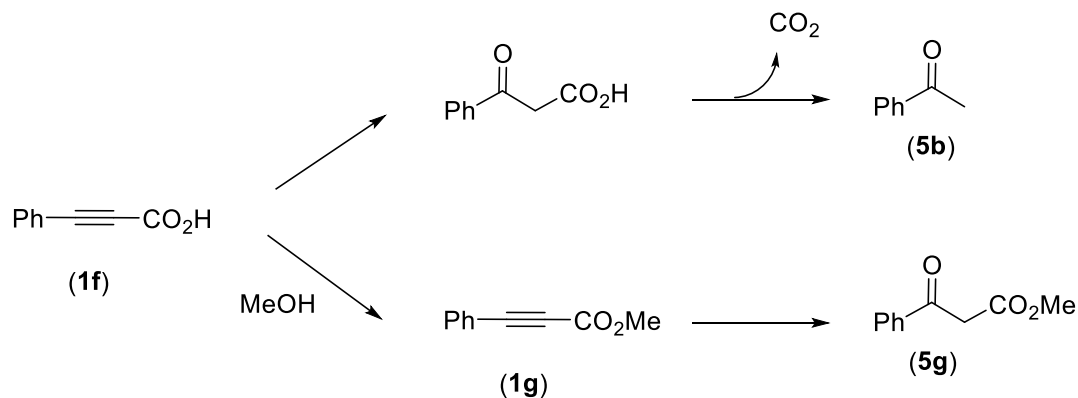
The number identifies the type of product and in particular: 3 for the vinyl ether, 4 for the acetal, and 5 for the hydration of the alkyne. The first letter accounts for the alkyne used in the catalytic test (a: ethyl phenylpropionate; b: phenylacetylene; c: ethyl propiolate; d: 3-hexyne; e: diphenylacetylene; f: phenylpropionic acid), while the second represents the alcohol (a: MeOH; b: *n*BuOH; c: PhOH).

In the literature, it is reported that terminal alkynes usually present a better selectivity toward the vinyl ether, giving preferentially nucleophilic attack at the internal carbon. [35] This is clearly evident in the test with ethyl propiolate as the alkyne (Entry 5, Table 3): the vinyl ether 3ca (both in *Z* and *E* form) is preferentially formed at short reaction times, together with the other vinyl ether regioisomer 3ca'. Nonetheless, considering the high reactivity of terminal alkynes, the formation of the acetal is usually also observed [35]. In fact, acetal 4ca becomes the major product at longer reaction times. The formation of the acetal also clearly favors the subsequent reaction, giving the product of formal alkyne hydration. In the case of ethyl propiolate as the alkyne (Entry 5, Table 3), this product appeared only at long reaction times, while with phenylacetylene, 5b was the only product observed.

In the other two cases, the hydration product was the only one detected, namely with diphenylacetylene and 3-hexyne (Entries 6 and 7, Table 3). In the case of ethyl phenylpropionate,

the vinyl ethers were observed at short reaction times (1.5 h), but for a prolonged reaction time, the hydration product was found as the only product (Entries 1 and 2, Table 3). This trend was observed with methanol as the alcohol as well as with n-butanol.

A peculiar reactivity was finally observed in the case of phenylpropionic acid. In this case, the expected hydroalkoxylation products were observed more, though products **5b**, **5g**, and **1g** (Figure 3) were obtained in low to moderate yield. The formation of these compounds can be explained with the reactions reported in Scheme 3; the hydration of the alkyne **1f** affords benzoylacetic acid, $\text{PhC(O)CH}_2\text{C(O)OH}$, which upon decarboxylation gives product **5b**. Alkyne **1g** forms by esterification of the carboxylic acid of alkyne **1f**; its hydration gives product **5g**.



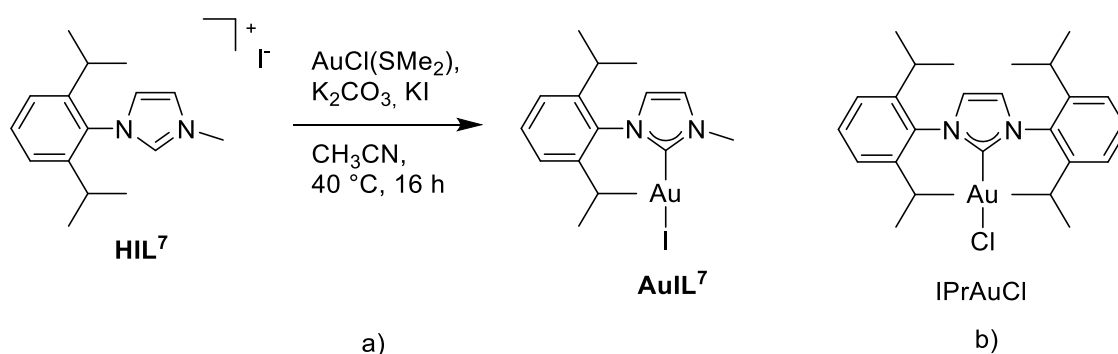
Scheme 3. Reaction accounting for the formation of products **1g**, **5b**, and **5g** in the hydromethoxylation of phenylpropionic acid.

The use of different silver salts may also influence not only the rate of the reaction, but also the product distribution. This is evident when comparing the results obtained in the reaction between diphenylacetylene and MeOH, using AgOTs or AgOTf as the co-catalyst (Entries 7 and 9, respectively in Table 3). In the case of AgOTs, the vinyl ether **3ea** is the main product after 1 h, and this can be ascribed to the different hygroscopic character of the used silver salts. AgOTs is in fact less hygroscopic than AgOTf, reducing the possible water content of the reaction mixture and thus allowing the identification of the olefin.

2.5. Comparison of The Catalytic Performances of $\text{Au}_2\text{Br}_2\text{L}^4$ with Mononuclear Catalysts

To evaluate the effect of the nuclearity of the complexes on the catalytic performance, we carried out the hydromethoxylation of 3-hexyne with two mononuclear complexes, namely the commercially available IPrAuCl and **AuIL**⁷. Complex **AuIL**⁷ is a new complex, prepared ad hoc for this study by treating the ligand precursor $\text{L}^7\cdot\text{HI}$ with $\text{AuCl}(\text{SMe}_2)$, using K_2CO_3 as base and KI (Scheme 4). Complex **AuIL**⁷ has been characterized by means of ^1H and ^{13}C NMR (Figures S1–S4), Electrospray Ionization–Mass Spectrometry (ESI-MS) and elemental analysis.

In the ^1H NMR spectrum of **AuIL**⁷, the absence of the signal relative to the proton in position 2 of the imidazolium ring (NCHN) is indicative of the formation of the carbene species. This is further supported by a ^{13}C NMR experiment where the resonance of the carbene carbon (NCN) was found at 183.5 ppm, a value consistent with the literature for NHC gold(I) complexes where an iodide is coordinated to the gold(I) center *trans* to the NHC ligand.



Scheme 4. (a) Synthesis of complex **AuIL**⁷. (b) The commercially available **IPrAuCl**.

The two mononuclear complexes were tested in the hydromethoxylation of 3-hexyne in the same condition employed for **Au₂Br₂L⁴** (Table 3), but using 2 mol% with respect to the alkyne to have the same amount of gold in the system. Complex **IPrAuCl** behaves better than **Au₂Br₂L⁴**, fully converting 3-hexyne after the first hour of reaction (Entry 1, Table 4). These results are in agreement with those reported by Zuccaccia et al. in the hydromethoxylation of 3-hexyne by using pre-formed **IPrAuOTf** as the catalyst [18]. In particular, the authors were able to completely convert the alkyne substrate by using 1.0 mol% of catalyst in chloroform at 50 °C in ca. 30 min, observing only the hydration product **5d**. In contrast, complex **AuIL**⁷ is totally inactive in the adopted reaction conditions, being unable to convert the substrate to any extent even after 18.5 h (Entry 2, Table 4). We also tested **AuIL**⁷ in the activation of ethyl-phenylpropiolate, but as in the case of 3-hexyne, we observed no reaction (Entry 3, Table 4). The three considered complexes (**IPrAuCl**, **AuIL**⁷, and **Au₂Br₂L⁴**) present different halides in the coordination sphere; the halide ligand is usually removed with the addition of a silver salt as a co-catalyst, which favors the formation of the active cationic species with concomitant precipitation of **AgX**. This reaction is usually considered fast and quantitative, so we believe that the effect of the different halides on the catalytic efficiency of the studied complexes is negligible. Furthermore, the reaction forming the active species is influenced by two factors: (i) the strength of the Au–X bond [38], and (ii) the solubility of the silver halide product, [39] both of which decrease along the halogen group. Thus, the removal of the iodide should be more favored than the removal of a bromide or a chloride. For these reasons, the results with the two mononuclear complexes highlight the crucial effect of the steric hindrance of the wingtip substituents of the ligand on the catalytic performance.

Table 4. Catalytic experiments performed with mononuclear gold(I) NHC complexes.

Entry	Alkyne	Alcohol	Cat (mol%)	Co-Cat (mol%)	T (°C)	T (h)	Alkyne Conversion (%) ^a
1	EtC≡CEt	MeOH	IPrAuCl (2)	AgOTf (2)	40	1	100
2	EtC≡CEt	MeOH	AuIL ⁷ (2)	AgOTf (2)	40	1 18.5	nr nr
3	PhC≡CCO ₂ Et	MeOH	AuIL ⁷ (2)	AgOTf (2)	40	1 18.5	nr nr

Reaction conditions: alkyne (0.6 mmol), MeOH (0.5 mL, 12.3 mmol), gold cat. (0.012 mmol), **AgOTf** co-cat. (0.012 mmol). ^a Alkyne conversion has been determined by ¹H NMR.

3. Materials and Methods

All manipulations were performed using standard Schlenk techniques under an atmosphere of argon. The reagents and the solvents were commercially available as high-purity products and generally used as received. The imidazolium salt 1-(2,6-diisopropylphenyl)-3-methylimidazolium iodide (**L**⁷·**HI**) and the dinuclear gold(I) complexes **Au₂Br₂L¹⁻²**-**Au₂Br₂L⁶⁻²** were prepared according to

the literature [34,40]. A Bruker Avance 300 MHz (300.1 MHz for ^1H ; 75.5 for ^{13}C) was used for NMR experiments; chemical shifts (δ) are reported in units of parts per million (ppm) relative to the residual solvent signals. ESI mass spectra were obtained by using a Finnigan Thermo LCQ-Duo ESI mass spectrometer. Elemental analyses were performed with a Thermo Scientific FLASH 2000 instrument at the Department of Chemical Sciences of the University of Padova.

3.1. Synthesis of the Mononuclear Gold(I) Complex $\{1-(2,6\text{-Diisopropylphenyl})\text{-3-Methylimidazol-2-Ylidene}\}\text{Iodogold(I) AuIL}^7$

A mixture of the imidazolium salt (0.15 mmol), $\text{AuCl}(\text{SMe}_2)$ (0.15 mmol), potassium carbonate (3.27 mmol), and KI (0.75 mmol) in acetonitrile (15 mL) was heated at 40 °C for 16 h. Subsequently, the obtained suspension was filtered over a 0.45 μm PTFE Millipore syringe filter. The reaction solvent was then removed under reduced pressure, obtaining a brown/yellow solid. Recrystallization from dichloromethane/*n*-hexane affords an orange/brown solid.

Yield 76%. ^1H NMR (300.13 MHz, CDCl_3 , 25 °C) δ ppm: 1.11 (d, $J = 6.8$ Hz, 6 H, CH_3), 1.28 (d, $J = 6.8$ Hz, 12 H, CH_3), 2.40 (sept, $J = 6.8$, 2H, CH *i*-Pr), 3.99 (s, 3H, CH_3), 6.92 (m, 1 H, CH_{im}), 7.14 (m, 1H, CH_{im}), 7.23 (m, 2 H, CH_{ar}), 7.46 (m, 1 H, CH_{ar}). ^{13}C NMR (75.48 MHz, CDCl_3 , 25 °C) δ ppm: 24.5 (2 CH_3), 28.5 (CH *i*-Pr), 38.2 (CH_3), 121.4 (CH_{im}), 123.3 (CH_{im}), 124.3 (CH_{ar}), 130.7 (CH_{ar}), 143.5 (N_{Car}), 145.9 (C_{ar}), 183.5 (C-Au). ESI-MS (positive ions, CH_3CN); m/z : 681.38 [$\text{M} - \text{I} + \text{L}^7$] $^+$. Elemental analysis calcd. for $\text{C}_{16}\text{H}_{22}\text{AuIN}_2$: C = 33.94%, H = 3.92%, N = 4.95%, Found: C = 34.10%, H = 3.95%, N = 4.89%.

3.2. X-ray Crystal Structure Determination of $\text{Au}_2\text{Br}_2\text{L}^4$

The crystallographic data for $\text{Au}_2\text{Br}_2\text{L}^4$ were collected on a APEX II Bruker CCD diffractometer. Unit-cell geometrical parameters and the data collection (20 s/frame scan time for a sphere of diffraction data) were obtained by using the APEX 3 program package [41], SAINT [41] and SADABS [42] were used to process the raw frame data to obtain the data file of the reflections. The structures were solved using SHELXT [43] (the Intrinsic Phasing method in the APEX 3 program). The refinement of the structures was performed using the SHELXTL-2014/7 program [44] in the WinGX suite v.2014.1 [45]. The hydrogen atoms were incorporated in the refinement in specified geometry and refined “riding” on the related carbon atoms.

Crystal data for the compounds are reported in Table S1. Crystallographic data were deposited with the Cambridge Crystallographic Data Centre as supplementary publication (CCDC 1968216). Copies of the data can be obtained free of charge on application to the CCDC, 12 Union Road, Cambridge CB2 1EZ, U.K. (fax, (+44) 1223 336033; e-mail, deposit@ccdc.cam.ac.uk).

3.3. Catalytic Tests on the Alkyne Hydroalkoxylation Reaction

A typical catalytic experiment was performed in a Schlenk tube equipped with a magnetic stirring bar. Initially, the gold(I) complex, the silver(I) salt co-catalyst, and the alkyne (if solid) were placed under an inert atmosphere. Then, the alcohol, the solvent (if present), and the alkyne (if liquid) were mixed and injected into the Schlenk tube. Subsequently, the reaction vessel was put in an oil bath warmed at the desired reaction temperature, and the mixture was stirred for the selected reaction time. The ^1H NMR experiment on a sample of the reaction mixture diluted in CDCl_3 , following the addition of 1,4-bis(trimethylsilyl)benzene as an internal standard, was used to determine the conversions and yields.

4. Conclusions

In this work, we studied the catalytic activity of a family of six dinuclear gold(I) complexes of general formula $\text{Au}_2\text{Br}_2\text{L}$ (L = diNHC) in the hydroalkoxylation of alkynes reaction.

In particular, we studied the effect of the molecular structure of the ligand on the catalytic performances of the complexes. In this frame, we observed that the best catalyst, $\text{Au}_2\text{Br}_2\text{L}^4$, was characterized by a ligand with bulky 2,6-diisopropylphenyl wingtip substituents and a methylene

bridging group between the two carbene donors. This combination afforded an enhanced stability to the complex in the reaction environment. Incidentally, $\text{Au}_2\text{Br}_2\text{L}^4$ has been previously reported to be the only catalyst of the series that is able to operate under harsh reaction conditions in the alkyne hydroamination reaction [34]. This finding suggests that in the case of the hydroalkoxylation of alkynes catalyzed by dinuclear gold(I) complexes, the ligand ability in stabilizing the catalyst active form has a big impact on the performance, whereas promotion of cooperative effects has a minor effect in connection to this reaction. On the basis of the results obtained in this and in our previous studies [34], the ligand effect in stabilizing the active catalytic species can be ranked as follows: $\text{L}^4 > \text{L}^6 \approx \text{L}^5 > \text{L}^1 \approx \text{L}^2 \approx \text{L}^3$. Complex $\text{Au}_2\text{Br}_2\text{L}^4$ was structurally characterized for the first time in this study, showing the presence of intramolecular aurophilic interactions in the solid state. The reaction scope was extended to both terminal and internal alkynes, with $\text{Au}_2\text{Br}_2\text{L}^4$ achieving fairly good conversions with challenging substrates such as diphenylacetylene. The activity of $\text{Au}_2\text{Br}_2\text{L}^4$ was compared with that of two mononuclear gold(I) NHC complexes: AuIL^7 , a mononuclear analog of complex $\text{Au}_2\text{Br}_2\text{L}^4$, and IPrAuCl , a commercially available benchmark catalyst. AuIL^7 was found to be totally inactive, while IPrAuCl performed much better than $\text{Au}_2\text{Br}_2\text{L}^4$. This comparison highlights once more the beneficial effect of using sterically encumbered ligands in the gold(I) catalyzed hydroalkoxylation of alkynes.

Supplementary Materials: The following are available online at <http://www.mdpi.com/2073-4344/10/1/1/s1>, NMR spectra of compound AuIL^7 ; Crystallographic data of compound $\text{Au}_2\text{Br}_2\text{L}^4$; Identification of the products of the alkyne hydroalkoxylation reactions; Product selectivity for the reactions reported in Table 2.

Author Contributions: Conceptualization, M.B., A.B., and C.T.; Validation, M.B. and C.T.; Formal analysis, E.M.; Investigation, E.M., M.B., and C.G.; Data curation, E.M. and M.B.; Writing—original draft preparation, M.B. and C.T.; Writing—review and editing, all authors; Visualization, M.B.; Supervision, M.B. and C.T. All authors have read and agreed the published version of the manuscript. All authors have read and agreed to the published version of the manuscript.

Funding: This research was funded by the University of Padova (DOR-DiSC).

Conflicts of Interest: The authors declare no conflicts of interest. The funders had no role in the design of the study; in the collection, analyses, or interpretation of data; in the writing of the manuscript, or in the decision to publish the results.

References

1. Teles, J.H.; Brode, S.; Chabanas, M. Cationic Gold(I) Complexes: Highly Efficient Catalysts for the Addition of Alcohols to Alkynes. *Angew. Chem. Int. Ed.* **1998**, *37*, 1415–1418. [CrossRef]
2. Huguet, N.; Echavarren, A.M. Gold-Catalyzed O–H Bond Addition to Unsaturated Organic Molecules. In *Hydrofunctionalization; Topics in Organometallic Chemistry*; Ananikov, V.P., Tanaka, M., Eds.; Springer: Berlin/Heidelberg, Germany, 2013; pp. 291–324. ISBN 978-3-642-33735-2.
3. Zhdanko, A.; Maier, M.E. Explanation of “Silver Effects” in Gold(I)-Catalyzed Hydroalkoxylation of Alkynes. *ACS Catal.* **2015**, *5*, 5994–6004. [CrossRef]
4. Corma, A.; Ruiz, V.R.; Leyva-Pérez, A.; Sabater, M.J. Regio- and Stereoselective Intermolecular Hydroalkoxylation of Alkynes Catalysed by Cationic Gold(I) Complexes. *Adv. Synth. Catal.* **2010**, *352*, 1701–1710. [CrossRef]
5. Veenboer, R.M.P.; Dupuy, S.; Nolan, S.P. Stereoselective Gold(I)-Catalyzed Intermolecular Hydroalkoxylation of Alkynes. *ACS Catal.* **2015**, *5*, 1330–1334. [CrossRef]
6. Ramón, R.S.; Pottier, C.; Gómez-Suárez, A.; Nolan, S.P. Gold(I)-Catalyzed Tandem Alkoxylation/Lactonization of γ -Hydroxy- α,β -Acetylenic Esters. *Adv. Synth. Catal.* **2011**, *353*, 1575–1583. [CrossRef]
7. Zhdanko, A.; Maier, M.E. The Mechanism of Gold(I)-Catalyzed Hydroalkoxylation of Alkynes: An Extensive Experimental Study. *Chem. Eur. J.* **2014**, *20*, 1918–1930. [CrossRef]
8. Larsen, M.H.; Houk, K.N.; Hashmi, A.S.K. Dual Gold Catalysis: Stepwise Catalyst Transfer via Dinuclear Clusters. *J. Am. Chem. Soc.* **2015**, *137*, 10668–10676. [CrossRef]
9. Hashmi, A.S.K. Dual Gold Catalysis. *Acc. Chem. Res.* **2014**, *47*, 864–876. [CrossRef]

10. Gómez-Suárez, A.; Nolan, S.P. Dinuclear Gold Catalysis: Are Two Gold Centers Better than One? *Angew. Chem. Int. Ed.* **2012**, *51*, 8156–8159. [[CrossRef](#)]
11. Tkatchouk, E.; Mankad, N.P.; Benitez, D.; Goddard, W.A.; Toste, F.D. Two Metals Are Better Than One in the Gold Catalyzed Oxidative Heteroarylation of Alkenes. *J. Am. Chem. Soc.* **2011**, *133*, 14293–14300. [[CrossRef](#)]
12. Hashmi, A.S.K.; Braun, I.; Nösel, P.; Schädlich, J.; Wieteck, M.; Rudolph, M.; Rominger, F. Simple Gold-Catalyzed Synthesis of Benzofulvenes—Gem-Diaurated Species as “Instant Dual-Activation” Precatalysts. *Angew. Chem. Int. Ed.* **2012**, *51*, 4456–4460. [[CrossRef](#)] [[PubMed](#)]
13. Hashmi, A.S.K.; Lauterbach, T.; Nösel, P.; Vilhelmsen, M.H.; Rudolph, M.; Rominger, F. Dual Gold Catalysis: σ,π -Propyne Acetylide and Hydroxyl-Bridged Digold Complexes as Easy-To-Prepare and Easy-To-Handle Precatalysts. *Chem. Eur. J.* **2013**, *19*, 1058–1065. [[CrossRef](#)]
14. Oonishi, Y.; Gómez-Suárez, A.; Martin, A.R.; Nolan, S.P. Hydrophenoxylation of Alkynes by Cooperative Gold Catalysis. *Angew. Chem.* **2013**, *125*, 9949–9953. [[CrossRef](#)]
15. Gómez-Suárez, A.; Oonishi, Y.; Martin, A.R.; Vummaleti, S.V.C.; Nelson, D.J.; Cordes, D.B.; Slawin, A.M.Z.; Cavallo, L.; Nolan, S.P.; Poater, A. On the Mechanism of the Digold(I)-Hydroxide-Catalysed Hydrophenoxylation of Alkynes. *Chem. Eur. J.* **2016**, *22*, 1125–1132. [[CrossRef](#)] [[PubMed](#)]
16. Casals-Cruañas, È.; González-Belman, O.F.; Besalú-Sala, P.; Nelson, D.J.; Poater, A. The preference for dual-gold(I) catalysis in the hydro (alkoxylation vs. phenoxylation) of alkynes. *Org. Biomol. Chem.* **2017**, *15*, 6416–6425. [[CrossRef](#)] [[PubMed](#)]
17. Zuccaccia, D.; Del Zotto, A.; Baratta, W. The pivotal role of the counterion in gold catalyzed hydration and alkoxylation of alkynes. *Coord. Chem. Rev.* **2019**, *396*, 103–116. [[CrossRef](#)]
18. Gatto, M.; Baratta, W.; Belanzoni, P.; Belpassi, L.; Zotto, A.D.; Tarantelli, F.; Zuccaccia, D. Hydration and alkoxylation of alkynes catalyzed by NHC–Au–OTf. *Green Chem.* **2018**, *20*, 2125–2134. [[CrossRef](#)]
19. Biasiolo, L.; Trinchillo, M.; Belanzoni, P.; Belpassi, L.; Busico, V.; Ciancaleoni, G.; D’Amora, A.; Macchioni, A.; Tarantelli, F.; Zuccaccia, D. Unexpected Anion Effect in the Alkoxylation of Alkynes Catalyzed by N-Heterocyclic Carbene (NHC) Cationic Gold Complexes. *Chem. Eur. J.* **2014**, *20*, 14594–14598. [[CrossRef](#)]
20. Trinchillo, M.; Belanzoni, P.; Belpassi, L.; Biasiolo, L.; Busico, V.; D’Amora, A.; D’Amore, L.; Del Zotto, A.; Tarantelli, F.; Tuzi, A.; et al. Extensive Experimental and Computational Study of Counterion Effect in the Reaction Mechanism of NHC-Gold(I)-Catalyzed Alkoxylation of Alkynes. *Organometallics* **2016**, *35*, 641–654. [[CrossRef](#)]
21. D’Amore, L.; Ciancaleoni, G.; Belpassi, L.; Tarantelli, F.; Zuccaccia, D.; Belanzoni, P. Unraveling the Anion/Ligand Interplay in the Reaction Mechanism of Gold(I)-Catalyzed Alkoxylation of Alkynes. *Organometallics* **2017**, *36*, 2364–2376. [[CrossRef](#)]
22. Biffis, A.; Baron, M.; Tubaro, C. Chapter Five—Poly-NHC Complexes of Transition Metals: Recent Applications and New Trends. *Adv. Organomet. Chem.* **2015**, *63*, 203–288.
23. Schmidbaur, H.; Schier, A. Auophilic interactions as a subject of current research: An up-date. *Chem. Soc. Rev.* **2011**, *41*, 370–412. [[CrossRef](#)] [[PubMed](#)]
24. Schmidbaur, H.; Schier, A. A briefing on auophilicity. *Chem. Soc. Rev.* **2008**, *37*, 1931–1951. [[CrossRef](#)] [[PubMed](#)]
25. Baron, M.; Tubaro, C.; Biffis, A.; Basato, M.; Graiff, C.; Poater, A.; Cavallo, L.; Armaroli, N.; Accorsi, G. Blue-Emitting Dinuclear N-heterocyclic Dicarbene Gold(I) Complex Featuring a Nearly Unit Quantum Yield. *Inorg. Chem.* **2012**, *51*, 1778–1784. [[CrossRef](#)]
26. Monticelli, M.; Tubaro, C.; Baron, M.; Basato, M.; Sgarbossa, P.; Graiff, C.; Accorsi, G.; Pell, T.P.; Wilson, D.J.D.; Barnard, P.J. Metal complexes with di(N-heterocyclic carbene) ligands bearing a rigid ortho-, meta or para-phenylene bridge. *Dalton Trans.* **2016**, *45*, 9540–9552. [[CrossRef](#)]
27. Tubaro, C.; Baron, M.; Costante, M.; Basato, M.; Biffis, A.; Gennaro, A.; Isse, A.A.; Graiff, C.; Accorsi, G. Dinuclear gold(I) complexes with propylene bridged N-heterocyclic dicarbene ligands: Synthesis, structures, and trends in reactivities and properties. *Dalton Trans.* **2013**, *42*, 10952–10963. [[CrossRef](#)]
28. Longhi, A.; Baron, M.; Rancan, M.; Bottaro, G.; Armelao, L.; Sgarbossa, P.; Tubaro, C. Possible Synthetic Approaches for Heterobimetallic Complexes by Using nNHC/tzNHC Heteroditopic Carbene Ligands. *Molecules* **2019**, *24*, 2305. [[CrossRef](#)]
29. Monticelli, M.; Baron, M.; Tubaro, C.; Bellemin-Laponnaz, S.; Graiff, C.; Bottaro, G.; Armelao, L.; Orian, L. Structural and Luminescent Properties of Homoleptic Silver(I), Gold(I), and Palladium(II) Complexes with nNHC-tzNHC Heteroditopic Carbene Ligands. *ACS Omega* **2019**, *4*, 4192–4205. [[CrossRef](#)]

30. Baron, M.; Tubaro, C.; Basato, M.; Isse, A.A.; Gennaro, A.; Cavallo, L.; Graiff, C.; Dolmella, A.; Falivene, L.; Caporaso, L. Insights into the Halogen Oxidative Addition Reaction to Dinuclear Gold(I) Di(NHC) Complexes. *Chem. Eur. J.* **2016**, *22*, 10211–10224. [[CrossRef](#)]
31. Baron, M.; Tubaro, C.; Basato, M.; Biffis, A.; Graiff, C. Synthesis of dinuclear N-heterocyclic dicarbene Au(III)/Au(III) and Au(II)/Au(II) complexes via oxidative addition of chlorine or bromine to Au(I)/Au(I) species. *J. Organomet. Chem.* **2012**, *714*, 41–46. [[CrossRef](#)]
32. Baron, M.; Tubaro, C.; Basato, M.; Natile, M.M.; Graiff, C. Oxidative halogenation of dinuclear N-heterocyclic dicarbene gold(I) complexes. *J. Organomet. Chem.* **2013**, *723*, 108–114. [[CrossRef](#)]
33. Mageed, A.H.; Skelton, B.W.; Sobolev, A.N.; Baker, M.V. Formation of Dinuclear AuII and AuI/AuIII Mixed-Valence Complexes is Directed by Structural Constraints Imposed by Cyclophane-NHC Ligands. *Eur. J. Inorg. Chem.* **2018**, *1*, 109–120. [[CrossRef](#)]
34. Baron, M.; Battistel, E.; Tubaro, C.; Biffis, A.; Armelao, L.; Rancan, M.; Graiff, C. Single-Step Synthesis of Dinuclear Neutral Gold(I) Complexes with Bridging Di(N-heterocyclic carbene) Ligands and Their Catalytic Performance in Cross Coupling Reactions and Alkyne Hydroamination. *Organometallics* **2018**, *37*, 4213–4223. [[CrossRef](#)]
35. Goodwin, J.A.; Aponick, A. Regioselectivity in the Au-catalyzed hydration and hydroalkoxylation of alkynes. *Chem. Commun.* **2015**, *51*, 8730–8741. [[CrossRef](#)] [[PubMed](#)]
36. Heidrich, M.; Bergmann, M.; Müller-Borges, D.; Plenio, H. Bispentipicyenyl-N-Heterocyclic Carbene (NHC) Gold Complexes: Highly Active Catalysts for the Room Temperature Hydration of Alkynes. *Adv. Synth. Catal.* **2018**, *360*, 3572–3578. [[CrossRef](#)]
37. Sirindil, F.; Nolan, S.P.; Dagonne, S.; Pale, P.; Blanc, A.; de Frémont, P. Synthesis, Characterization and Catalytic Activity of NHC Gold(I) Polyoxometalate Complexes. *Chem. Eur. J.* **2018**, *24*, 12630–12637. [[CrossRef](#)]
38. Flahaut, A.; Roland, S.; Mangeney, P. Allylic alkylation and amination using mixed (NHC) (phosphine) palladium complexes under biphasic conditions. *J. Organomet. Chem.* **2007**, *692*, 5754–5762. [[CrossRef](#)]
39. Brown, J.R.; Schwerdtfeger, P.; Schröder, D.; Schwarz, H. Experimental and theoretical studies of diatomic gold halides. *J. Am. Soc. Mass Spectrom.* **2002**, *13*, 485–492. [[CrossRef](#)]
40. Waghorne, W.E. Solubilities of the Silver Halides in Aqueous Mixtures of Methanol, Acetonitrile, and Dimethylsulfoxide. *Mon. Chem.* **2003**, *134*, 655–667. [[CrossRef](#)]
41. Bruker. *APEX3 and SAINT*; Bruker AXS Inc.: Madison, WI, USA, 2015.
42. Krause, L.; Herbst-Irmer, R.; Sheldrick, G.M.; Stalke, D. Comparison of silver and molybdenum microfocus X-ray sources for single-crystal structure determination. *J. Appl. Crystallogr.* **2015**, *48*, 3–10. [[CrossRef](#)]
43. Sheldrick, G.M. SHELXT—Integrated space-group and crystal-structure determination. *Acta Crystallogr. Sect. Found. Adv.* **2015**, *71*, 3–8. [[CrossRef](#)] [[PubMed](#)]
44. Sheldrick, G.M. Crystal structure refinement with SHELXL. *Acta Crystallogr. Sect. C Struct. Chem.* **2015**, *71*, 3–8. [[CrossRef](#)] [[PubMed](#)]
45. Farrugia, L.J. WinGX and ORTEP for Windows: An update. *J. Appl. Crystallogr.* **2012**, *45*, 849–854. [[CrossRef](#)]



© 2019 by the authors. Licensee MDPI, Basel, Switzerland. This article is an open access article distributed under the terms and conditions of the Creative Commons Attribution (CC BY) license (<http://creativecommons.org/licenses/by/4.0/>).